ACI MATERIALS JOURNAL TECHNICAL PAPER

Title no. 99-M2

Flexural Behaviors of Glass Fiber-Reinforced Polymer (GFRP) Reinforced Engineered Cementitious Composite Beams

by Victor C. Li and Shuxin Wang

Broad applications of fiber-reinforced polymer (FRP) reinforcement are hindered by its elastic brittle behavior, which results in reduced structural ductility. In addition, due to the lower modulus of elasticity, serviceability considerations such as deflection and crack width control present serious challenges to designers. This paper reports new means to address these issues by introducing engineered cementitious composite (ECC), which is designed based on micromechanics principles and exhibits higher tensile and shear ductility, to replace brittle concrete matrix. Three series, totaling 16 GFRP reinforced beams with various shear span-depth ratios and longitudinal reinforcement ratios, were tested. The results reveal that, under the same reinforcement configurations, ECC beams exhibit significant increases in flexural performance in terms of ductility, load-carrying capacity, shear resistance, and damage tolerance (such as crack width or spalling) compared with the counterpart high-strength concrete (HSC) beam. The extent of improvement strongly depended on the failure mode; that is, when the limit state was dominated by matrix behavior, more significant improvement was observed. Moreover, ECC beams without shear reinforcement demonstrate better performance than HSC beams with dense steel stirrups, which suggests that elimination of shear reinforcement is feasible when the concrete matrix is replaced by ECC.

Keywords: beam; ductility; reinforcement; shear.

INTRODUCTION

FRP composite made with resin-impregnated continuous fibers is considered a promising alternative to the traditional steel reinforcements because of its inherent corrosive resistance, though the long-term performance of some types of fiber in certain environments is still questionable. Other appealing characteristics of FRP include high tensile strength, good fatigue and damping response, high strength-to-weight ratio, and electromagnetic transparency. The wide-ranging application of FRP reinforcements, especially as a main reinforcement, however, has been rather limited. This may be partially attributed to the high initial cost of materials and the lack of design guidelines, but more essentially can be attributed to two major engineering drawbacks of FRP materials: low modulus of elasticity and the lack of ductility of most commercially available FRPs.

FRP generally exhibits a linear elastic tensile stress-strain relationship up to failure which, in comparison to steel-reinforced members, may result in poor structural ductility even in properly designed (according to standard reinforced concrete design guidelines) FRP-reinforced members. Essentially, ductility is the ability of inelastic energy dissipation. For conventional steel-reinforced concrete members, ductility is primarily achieved by the yielding of steel reinforcement, thus consuming a substantial amount of energy while allowing the full compressive strain capacity of the concrete to develop. For an FRP-reinforced concrete member, however, such an inelastic energy consumption mechanism does not exist. The main source of inelastic energy dissipation therefore comes from the cracking and crushing of the concrete matrix. Debonding and slippage between reinforcement and matrix also consume a certain portion of energy, but this portion is rather small due to the low reinforcement ratio in practically-used structural members. In seismic zones, although FRP-reinforced concrete members may perform large deformations, the energy dissipation is very little.[1] Since the structural failure due to FRP reinforcing bar rupture is rather catastrophic, the over-reinforced design concept that ensures that compressive failure of concrete takes place prior to the tensile failure of FRP has been well accepted.[2-4] Nanni pointed out that, for FRP-reinforced concrete beams, the balanced reinforcement ratio, which is defined as the reinforcement ratio producing a condition for simultaneous failure of the concrete and the FRP reinforcing bar, is much lower than the practically adopted reinforcement ratio if the concrete is unconfined.[5] To fully develop the strain capacity of FRP reinforcement and also to gain plastic deformability, HSC and effective confinement at the compressive zone such as intensive stirrups or spirals should be used. In 1995, Naaman proposed to use slurry-infiltrated fiber concrete (SIFCON), a kind of steel fiber-reinforced mortar with a high fiber-volume fraction, to improve the ductility of FRP prestressed beam. Substantial ductility was achieved by forming a plastic hinge at the compression zone.[6] Efforts were also made to develop new types of ductile hybrid FRP composites with deliberately designed fiber architecture.[7-8]

Except for carbon fiber-reinforced polymer (CFRP), the modulus of elasticity of most available FRP materials is only 1/5 to 1/3 that of steel, which results in larger deflections as well as larger crack widths under service loads in comparison with those of its counterpart steel-reinforced concrete element for a given reinforcement ratio.[9-12] Serviceability criteria, therefore, rather than strength criteria, would govern the design of FRP-reinforced concrete members. Since corrosion is not an issue with FRP reinforcing bars, crack width control would be based mainly on aesthetic consideration rather than on durability concerns. In applications such as water-retaining structures, where permeability control is a key issue, however, maximum crack width has to be limited.

For conventional steel-reinforced concrete elements, shear failure is a more serious problem than flexural failure. This is also true for FRP-reinforced concrete elements. In these elements, shear resistance contributed from aggregate

ACI Materials Journal, V. 99, No. 1, January-February 2002.
MS No. 01-043 received February 19, 2001, and reviewed under Institute publication policies. Pertinent discussion will be published in the November-December 2002 *ACI Materials Journal* if received by August 1, 2002.

ACI member **Victor C. Li** *is a professor of civil and environmental engineering at the University of Michigan, Ann Arbor, Mich. His research interests include micromechanics-based composite materials design and engineering, and innovative structural design based on advanced materials technology and infrastructure engineering.*

ACI member **Shuxin Wang** *is a graduate student research assistant in the Department of Civil and Environmental Engineering at the University of Michigan. He received his BS and MS from Tsinghua University, Beijing, China. His research interests include the development of engineered cementitious composites and the application of fiber-reinforced plastic reinforcement.*

Table 1—GFRP reinforcing bar properties

Bar size designation		Tensile modulus of elasticity	Ultimate tensile strength	Allowable tensile stress (working stress limit)	Ultimate strain in tension
	mm	E_f, GPA	F_u, MPa	$f_{c.a}$, MPa	ε_{fu}, %
No. 4	12.9	40	740	185	1.9

Fig. 1—GFRP reinforcing bar.

interlock is usually diminished due to larger crack width. In addition, the dowel effect of FRP longitudinal bars is lower than that of steel reinforcement, because the brittle fibers are rather sensitive to transverse stress concentrations. To completely resolve the corrosion problem, it is preferable to eliminate the use of steel reinforcement, including stirrups. Two problems arise when FRP is also used as shear reinforcement: first, most FRP materials are made of thermoset resin and brittle fibers, thus shaping of stirrups has to be done before resin cure; second, significant strength reductions (as high as 40%) at the location of the bents were observed for FRP-made stirrups, which suggests that FRP is not an effective shear reinforcement.[13-14]

Based on micromechanical principles, ECC materials have been developed in recent years. ECC materials exhibit strain-hardening in tension with a remarkably high strain capacity (3.5 to 6%) and crack width control, while their compressive strengths are comparable to those of HSCs (60 to 90 MPa).[15] Associated with the strain-hardening behavior is the high fracture toughness of ECC, which reaches 30 KJ/m^2.[16-17] All of these high performances are achieved by using short fibers at moderate volume fractions, usually less than 2%. Unlike SIFCON, ECC exhibits isotropic mechanical properties, and can be prepared by normal mixing processing. These unique properties make ECC promising for work in conjunction with FRP to enhance structural ductility and serviceability. Recent studies on the structural performance of steel-reinforced beam elements with ECC show that the brittle failures, such as shear fracture and bond splitting failure, observed in RC beams can be prevented by using ECC in place of the concrete, thereby validating the feasibility of upgrading the structural performance and damage tolerance of structural elements via ECC materials.[18] In addition, the interest in using FRP reinforcement in lieu of traditional steel reinforcement mainly lies in the durability of FRP-reinforced structural members in aggressive environments. Synthetic fiber may be more desirable than steel fiber when choosing an appropriate FRC material in combination with FRP main reinforcement.

This paper reports the experimental results on the flexural and shear behavior of GFRP-reinforced ECC beams. For comparison, behaviors of counterpart GFRP-reinforced HSC beams are also presented. The investigation was focused on the following targets: utilizing the shear capacity of ECC material to reduce or even eliminate the shear reinforcement, thus enhancing the deformability and ductility of FRP-reinforced beams and controlling crack width. A total of 16 simple rectangular beams were tested, which were classified into three series according to different targeted failure modes. These failure modes are: shear failure, flexural failure in tension, and flexural failure in compression. The failure modes, load-carrying capacities, deformabilities, ductilities, and crack widths are reported.

RESEARCH SIGNIFICANCE

This paper presents an alternative approach to improve the ductility and serviceability of FRP-reinforced structural members by replacing the brittle concrete matrix with a fiber-reinforced cementitious composite with strain-hardening behavior (ECC material). Results from beam flexural bending tests show considerable improvement in terms of energy dissipation ratio, load-carrying capacity, shear resistance, crack width, and damage level. These findings provide preliminary insights into the interaction between the ductile matrix (in tension) and brittle reinforcement, and are useful in improving the overall performance of FRP-reinforced structural elements.

EXPERIMENTAL PROGRAM

Material properties

Reinforcements—The FRP reinforcing bars used in this investigation are E-GFRP rods. As shown in Fig. 1, the reinforcing bar has spiral-wrapped glass fiber braid to provide lateral confinement, and a coarse silica sand-coated surface to enhance bonding with the concrete matrix. The mechanical and design properties of this GFRP rod are given in Table 1. Like most other FRP reinforcing bars, this GFRP rod exhibits linear elastic behavior up to brittle failure.

A regular Grade 60 deformed steel reinforcing bar with a yield strength of 410 MPa was used in the control beam for longitudinal reinforcement. The shear reinforcement adopted Grade 60 wire with a diameter of 5 mm. The same wire was also used for the compressive reinforcement.

Matrix—ECC materials are a class of short-fiber, randomly distributed cementitious composites with low fiber content designed based on micromechanical principles. The matrix toughness, interfacial bond, and characteristic parameters of the fibers in ECCs are tailored according to the models of crack growth micromechanics in a brittle matrix composite, whereby crack bridging is provided by fibers to achieve steady state cracking.[19-20] The ECC material used in this investigation is polyethylene ECC with 1.5% fiber volume fraction. The polyethylene fiber has a diameter of 38 μm and a length of 12 mm. The modulus of elasticity and tensile strength of this fiber are 120 GPa and 2700 MPa, respectively. For the concrete beams, HSC with a nominal compressive strength of 67 MPa was used. Mixture constituents include 9.5 mm maximum size coarse aggregate, Type 2NS fine aggregate, and Type I portland cement. The same cement was also used in the ECC mixture. Table 2 gives the mixture proportions of these two matrixes.

Table 2—Matrix proportions

Matrix designation	Cement	Sand	Coarse aggregate	Water	High-range water-reducing admixture, %	Hydroxylpropyl methylcellulose, %	Antifoamer, %	Polyethylene fiber, %
Concrete	1	1.7	1.7	0.42	0.6	—	—	—
ECC	1	0.5	—	0.28	4.0	0.05	0.05	1.5

Table 3—Summary of beam specimens

Series	Beam designation	Length L, mm	Longitudinal reinforcement	Longitudinal reinforcement ratio, %	Shear reinforcement*	Matrix type	Matrix f_c', MPa
I	SRC10	1017	Steel reinforcing bar 3 No. 3	1.47	Stirrups @ 38 mm	Concrete	68.5
	GRC10-ns		GFRP reinforcing bar 2 No. 4	1.82	—	Concrete	65.3
	GRC10				Stirrups @ 38 mm	Concrete	65.8
	GRE10-ns†				—	ECC	71.8
	GRE10†				Stirrups @ 38 mm	ECC	71.8
II	GRC16	1600	GFRP reinforcing bar 2 No. 4	1.82	Stirrups @ 40 mm	Concrete	65.3
	GRE16-ns				—	ECC	78.4
	GRE16†				Stirrups @ 40 mm	ECC	71.2
III	GRC16-3R	1600	GFRP reinforcing bar 3 No. 4	2.73	Stirrups @ 40 mm	Concrete	66.0
	GRE16-3R-ns†				—	ECC	78.4
	GRE16-3R†				Stirrups @ 45 mm	ECC	76.2

*All stirrups made from smooth steel with diameter of 4.6 mm and yield strength of 460 MPa.
†Two identical beams were tested.

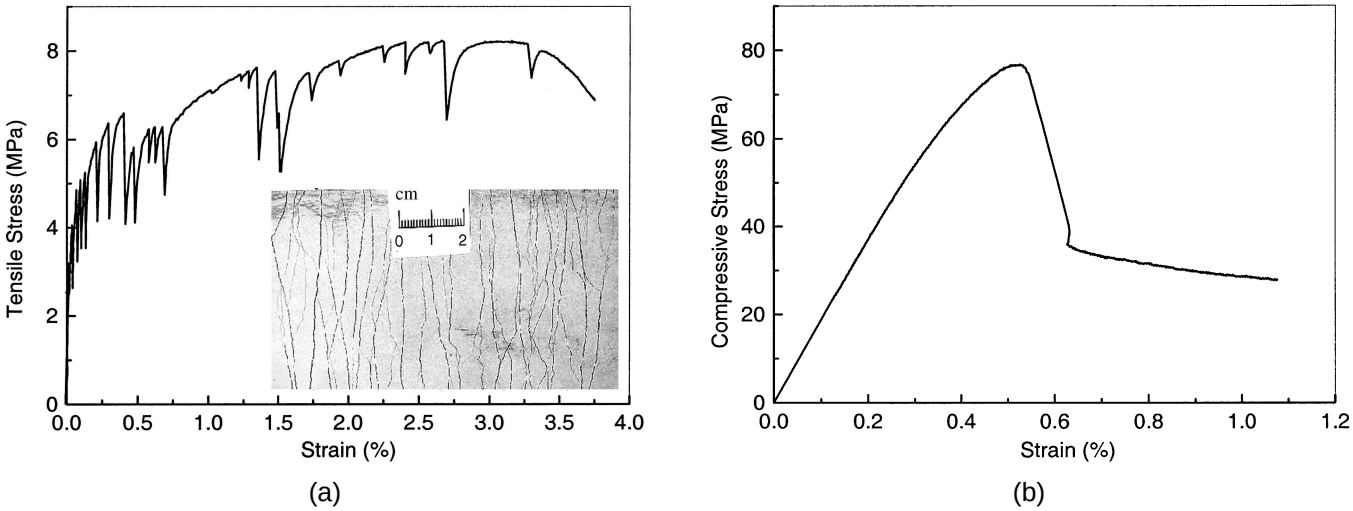

Fig. 2—(a) Tensile and (b) compressive stress-strain relationships of ECC matrix.

The tensile behavior of ECC material obtained from direct tensile test using plate specimen is shown in Fig. 2(a). Details of direct tensile test can be found in Li.[21] After first cracking, ECC strain-hardens like ductile metal, accompanied by multiple cracking and load-capacity increase. A first crack strength of 3 MPa, an ultimate tensile strength of 8.0 MPa, and a strain capacity of 3.5% were reached in this case. ECC can be tailored to accommodate property demands for different applications. Tensile strain capacity as high as 8% has been achieved.[15] Figure 2 shows the compressive stress-strain relationship of ECC material. Compared with that of HSC, ECC exhibits high ultimate strain capacity and a long post-peak softening branch.

Test specimens

Eleven different types, totaling 16 beams, including five duplications, were tested. Targeting different failure modes, these beams are categorized into three series as detailed in Table 3. All the beams have same cross-sectional dimension (114 x 152 mm). Series I is composed of short beams with a length of 1017 mm, designed to fail in shear. Series II has the same reinforcement layout as Series I, but a longer length of 1600 mm, designed to fail in flexural tension. Series III is similar to Series II, except for a higher longitudinal reinforcement ratio, designed to fail in flexural compression. Each series includes at least one GFRP-reinforced concrete beam and two ECC beams. Regular steel wire was used for shear reinforcement (stirrups). The same wire was also placed longitudinally at the compressive zone to provide support for the stirrups.

The concrete beam is featured with crowded stirrups to provide maximum shear resistance and confinement in the compressive zone. In addition to the HSC matrix, these concrete beams are designed to fully develop their load-carrying

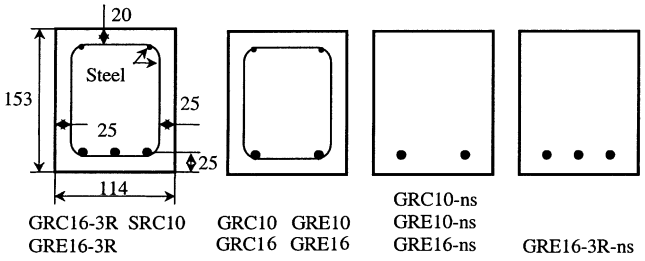

Fig. 3—Beam cross section details.

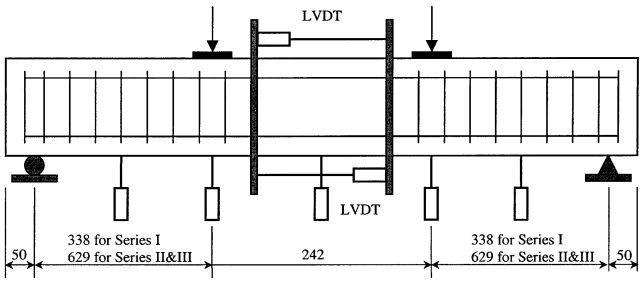

Fig. 4—Schematic of test setup.

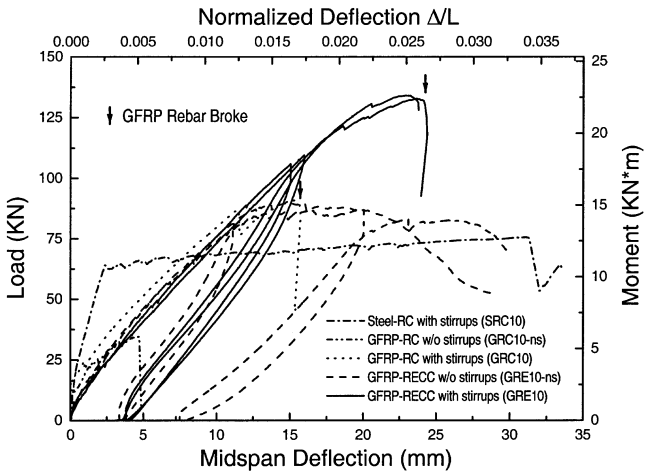

Fig. 5—Experimental load-deflection curves for Series I.

capacity. For the two ECC beams, GRE10 has identical reinforcement as the concrete beam GRC10 for investigating the influence of the matrix under different failure modes, while the steel stirrups are totally eliminated in another beam GRE10-ns. Beam SRC10 in Series I is a regular steel-reinforced concrete beam, designed according to ACI 318-95,[22] satisfying an under-reinforced condition, and is used as a reference. The compressive strength of the matrixes are also listed in Table 3, which shows that the ECC has a slightly higher, but comparable, compressive strength than the concrete matrix.

The details of the beam cross sections are illustrated in Fig. 3. The balanced reinforced ratio of those GFRP-reinforced beams, if calculated based on a compressive strain capacity of 0.0035 for unconfined concrete, is 1.08%. Therefore, all the GFRP-reinforced beams should be classified as over-reinforced. Since the concrete in the compressive zone is well-confined and the ECC material processes higher compressive strain capacity than 0.0035, however, the beams in Series I and II, which have a reinforcement ratio of 1.82, should be considered under-reinforced, as verified in the test.

All beams were cast in the laboratory and demolded after 24 h of moist curing. They were then sealed in plastic bags, cured in a 100%-humidity environment for 7 days, and left

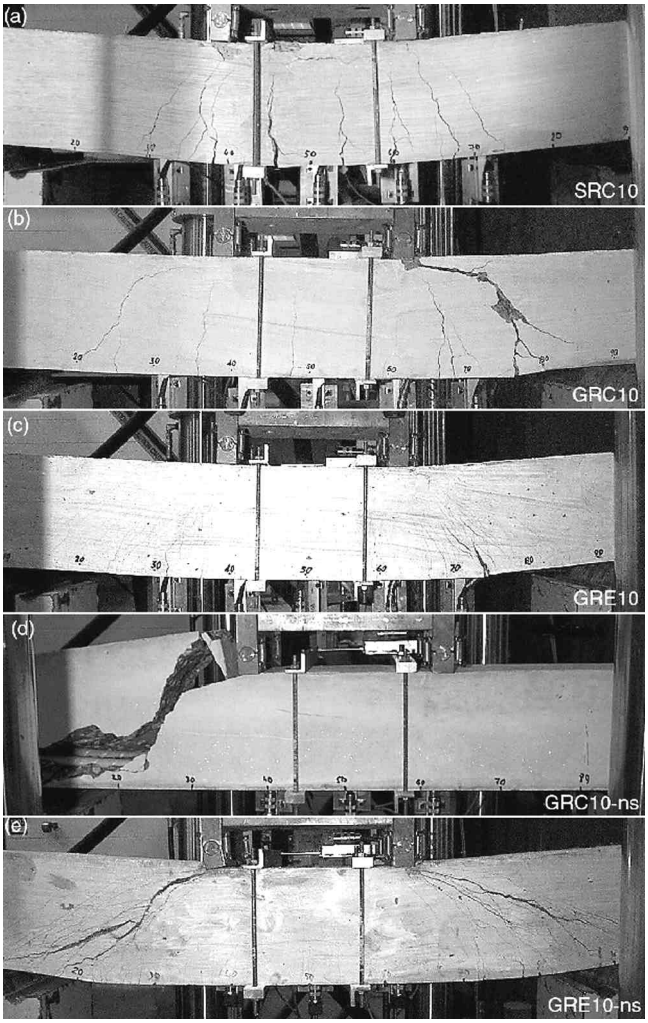

Fig. 6—Ultimate states of beam series I.

to air-dry until testing. The age at testing of the specimens was 28 days. Standard ϕ4 x 8 in. (ϕ101.6 x 203.2 mm) cylinder specimens for compression testing were also cast from the same matrix batch.

Test setup and test procedure

The schematic arrangement of the test setup is shown in Fig. 4. The beam was subjected to a four-point bending load. The distance of 242 mm between the two loading points is fixed for all three test series. The shear span-depth ratio for Series I is 2.62, whereas this ratio is increased to 4.88 for Series II and III. Five linear variable differential transformers (LVDTs) were used to monitor the deflection, and two other LVDTs attached to the top and bottom surfaces at the center span were used to measure the curvature in the constant moment segment. The load was applied under displacement control at the rate of 0.0254 mm/s. Except for beams GRC10 and GRC10-ns, which were monolithically loaded up to failure, the other beams experienced one cycle of the unloading and reloading process.

TEST RESULTS AND DISCUSSION

Deflection behaviors and failure modes

The experimental load versus midspan deflection curves of the three series specimens involved in this program as well as their ultimate states are given in Fig. 5 through 10.

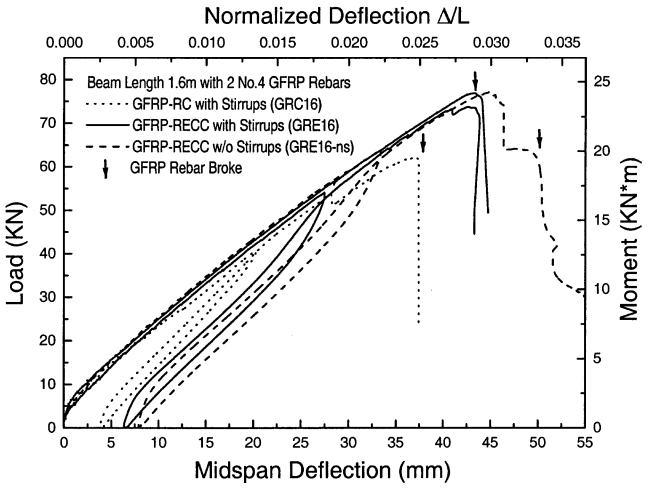

Fig. 7—Experimental load-deflection curves for Series II.

Normalized deflection in the figures refers to the ratio of midpoint deflection to span length between two reaction supports.

Series I

The steel-reinforced concrete beam SRC10, for which the tensile reinforcement ratio 1.47% is well below the balanced reinforcement ratio ρ_b = 4.3% for such sections, behaves very ductilely, as shown in Fig. 5 and Fig. 6(a). The first crack appeared in the center span at a load of 15.0 kN, then inclined shear cracks were induced beyond the pure moment span with increasing load. The main steel reinforcing bars yielded at a moment of 10.8 kN-m. After that, large deflection occurred with slightly increased moment. The beam finally failed in crushing and spalling of the concrete in the compression zone between the two load points, resulting in a sudden load drop. Shear failure was prevented by providing sufficient stirrups (ϕ5 mm stirrup @ 38 mm) in shear span, which was calculated according to ACI Building Code 318-95.

As has been confirmed by previous research,[3,4,8,9,23] concrete beams reinforced by GFRP reinforcing bars lack flexural rigidity and ductility due to the low elastic modulus and elastic behavior of FRP materials. Beam GRC10 has a similar reinforcement area to that of the reference beam SRC10, and the ultimate load capacity is also close; however, the load-deflection behaviors of these two beams are substantially different (Fig. 5). The first crack load of GRC10 is 14.8 kN, almost the same as that of SRC10. Beyond the cracking load, the flexural stiffness dropped but kept almost constant up to failure; no clear yielding plateau was observed. Only several diagonal shear cracks were developed in shear span, forming as extensions of flexural cracks. These shear cracks bent over to follow the compressive stress trajectory with increase of load, when two of them began to propagate along the longitudinal reinforcement. Due to the low shear span-effective depth ratio *a*/*d* (2.62 for this series), the beam flexural capacity cannot be fully developed, and the shear resistance dominates the ultimate load-carrying capacity. The failure of this beam was initiated by crushing and spalling of concrete at the top compression side of the main diagonal shear crack, which resulted in the kink on the load-deflection curve at a load of 86.9 kN, at which one of the main GFRP reinforcements broke and caused a sudden drop in load. The ultimate state of GRC10 is shown in Fig. 6(b).

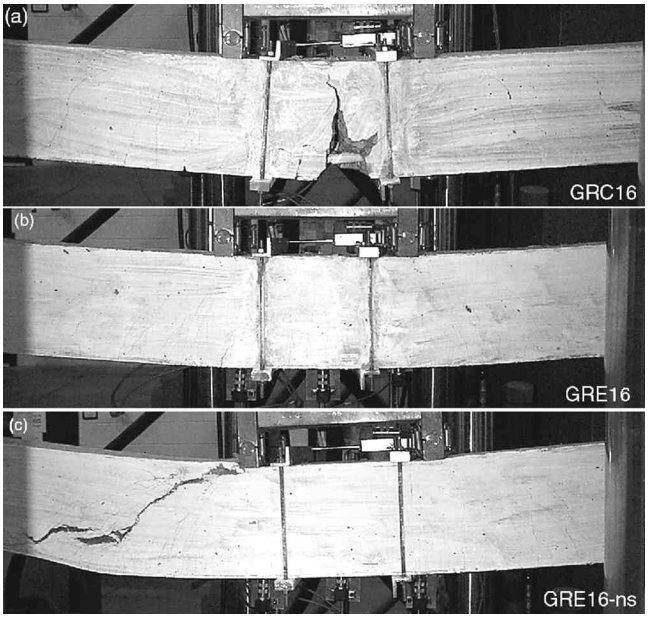

Fig. 8—Ultimate states of beam series II.

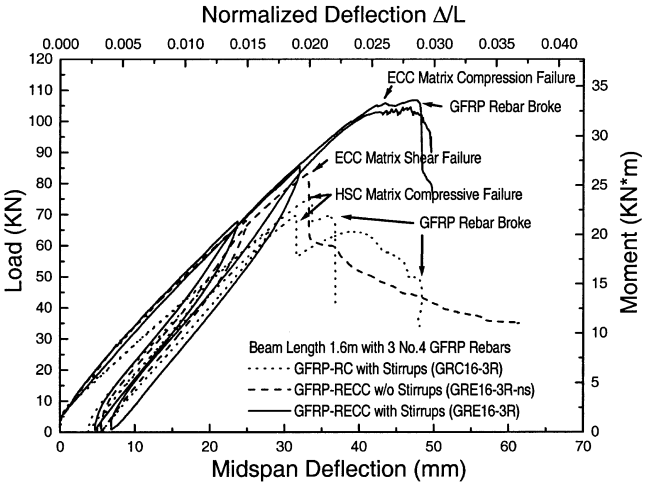

Fig. 9—Experimental load-deflection curves for Series III.

GRE10 has an identical reinforcement layout to that of GRC10, except a different matrix. Although these two beams behaved similarly before failure, GRE10 achieved a much larger load-carrying capacity, 46% higher than that of GRC10, as well as a significant improvement of 56% in ultimate deflection capacity (Fig. 5). The beam finally failed in shear-tension as shown in Fig. 6(c). The rupture of GFRP rod at the location of the main shear crack led to a sudden drop in load.

GRC10-ns and GRE10-ns are a pair of counterpart beams without steel shear reinforcement corresponding to GRC10 and GRE10. GRE10-ns exhibited similar load-deflection behavior to that of GRC10 before failure in shear. Very differently from the commonly known brittle mode of shear failure, however, the shear failure of GRE10-ns was considerably ductile. This behavior is due to the strain-hardening properties of the ECC matrix. In the initial stage, vertical flexural cracks appeared at the tensile side of the pure moment span. When the principle tensile stress within the shear span exceeded the first crack strength of the ECC matrix, a diagonal crack propagated through the beam web. Instead of only forming several

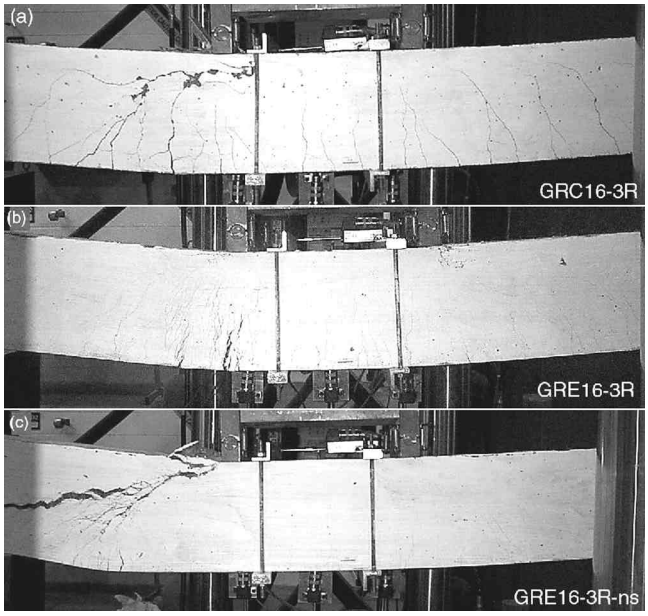

Fig. 10—Ultimate states of beam series III.

big cracks, as is usually the case in concrete beams, numerous small cracks developed in the ECC beams and spread throughout a large area. The bridging force carried by fibers across the cracks provided significant shear resistance, and the multiple cracking ensured the large deformation capacity. The load-deflection curve in Fig. 5 shows a plateau similar to the yielding process. Some kind of pseudoyielding ductility was achieved by extensive shear deformation. When the load capacity gently decayed to 85% of peak load, the GFRP reinforcing bars were still undamaged. After unloading, the center span looked intact due to the elastic behavior of the GFRP reinforcing bars. The peak load capacity of GRE10-ns was 86.9 kN, comparable to that of an equivalent concrete beam with intensive steel shear reinforcement (GRC10) wherein the deflection capacity increased by nearly 100%. Compared with the ductile shear failure of GRE10-ns, the shear failure of GRC10-ns is rather catastrophic. The propagation of shear cracks along the longitudinal reinforcing bar towards the support points quickly destroyed the integrity of beam, as shown in Fig. 6(d). The load-carrying and deflection capacities only reach 40 and 16%, respectively, of that of GRE10-ns.

Series II

The beams in Series II have the same reinforcement ratio as those in Series I, but longer shear spans. As a result, for beams GRC16 and GRE16 with steel shear reinforcement, the failure modes are controlled by flexural bending, whereas GRE16-ns retains shear failure. The load-deflection curves of these three beams up to failure, as shown in Fig. 7, are approximately identical. As mentioned previously, according to the ACI code, GRC16 should be categorized as an over-reinforced beam. In fact, corresponding to the kink on the load-deflection curve at a load of 55 kN, compressive cracks began to develop at extreme compressive fibers at midspan, prior to reaching the peak load. Since the core concrete is well-confined by the stirrups, however, the structural instability was actually caused by the rupture of the GFRP reinforcing bar rather than the compressive failure of the concrete. Consequently, this beam should still be considered an under-reinforced beam. The catastrophic rupture of the reinforcing bar led not only to a sudden drop in load capacity, but also to severe concrete spalling due to the release of elastic energy, as shown in Fig. 8(a).

The counterpart ECC beam GRE16 (Fig. 8(b)) also failed in flexural tension, but with moderately increased load-carrying and deformation capacities in comparison with the GRC16. This improvement may be attributed to the following aspects: contribution from fiber bridging; higher compressive stress-strain capacity of the ECC material; and more importantly, that the smeared crack distribution reduced the strain concentration on the reinforcing bar across the crack face and therefore delayed the reinforcing bar's rupture. The last aspect will be discussed further in the following section. While the steel shear reinforcement was totally eliminated, beam GRE16-ns reached nearly the same load capacity as beam GRE16. The failure mode, however, became shear-controlled. For these ECC beams, although the improvements in deformability and ductility are moderate, there is an essential difference in crack width control. ECC beams, GRE16 and GRE16-ns, developed much smaller crack widths than did Beam GRC16, which will be discussed in detail in the following section.

Series III

With higher longitudinal reinforcement ratios, Beams GRC16-3R and GRE16-3R with shear reinforcement fail in flexural compression. The stiffness of ECC beams in this series was found to be slightly higher than equivalent concrete beams due to the contribution of fiber bridging. This trend was not obvious in Series II. For the concrete Beam GRC16-3R (Fig. 10(a)), the spalling caused by matrix compressive failure led to a big loss in load capacity, though it was partially recovered later because of the intensive confinement on the concrete core. Such structural instability caused by matrix spalling, which is also observed on another concrete beam, GRC16, is unlikely to happen on ECC beams. Benefitting from the relatively ductile postpeak behavior under compression (Fig. 2(b)), the failure process of ECC in the compressive zone is rather gentle, manifested by the short plateau at the peak load on the load-deflection curve of Beam GRE16-3R. Compared with GRC16-3R, GRE16-3R (Fig. 10(b)) shows more than 50% improvement in both peak load and corresponding deflection. Moreover, it is reasonable to postulate that for higher reinforcement ratios, which usually occur in the field, to satisfy the stiffness requirement, the pseudoyielding plateau due to the ductile post-peak behavior of ECC material would be prolonged.

Similar to the result of Series II, the ECC beam with no shear reinforcement GRE16-3R-ns (Fig.10(c)) demonstrated a slightly larger load-carrying capacity than its counterpart concrete beam with crowded stirrups. Therefore, for the beams of the tested geometry with shear span-depth ratio from 2.6 to 4.9, it is fair to assert that, when the HSC matrix is replaced by ECC material, crowded shear reinforcement may be avoided. This implies not only improvement in structural durability, but also significant reduction in labor and time costs. Furthermore, as demonstrated in Series I, the shear failure of the beam with short shear span exhibits pseudoyielding behavior rather than the commonly-known brittle mode of shear failure, thus the structural ductility is enhanced.

Crack width and pattern

Due to the lower modulus of elasticity of GFRP-reinforcement (20% that of steel), resulting in reduced flexural

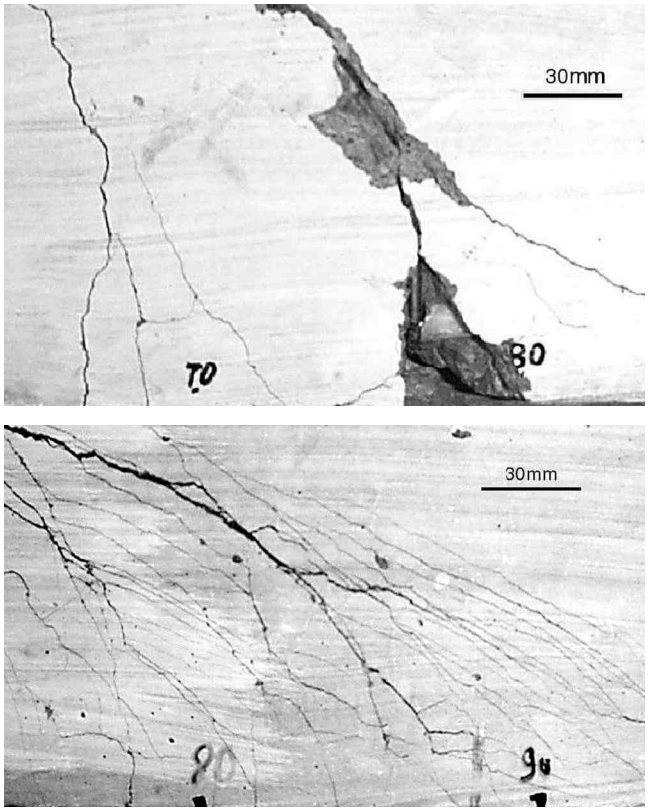

Fig. 11—Shear crack patterns of: (a) GFRP-reinforced concrete beam; and (b) GFRP-reinforced ECC beam.

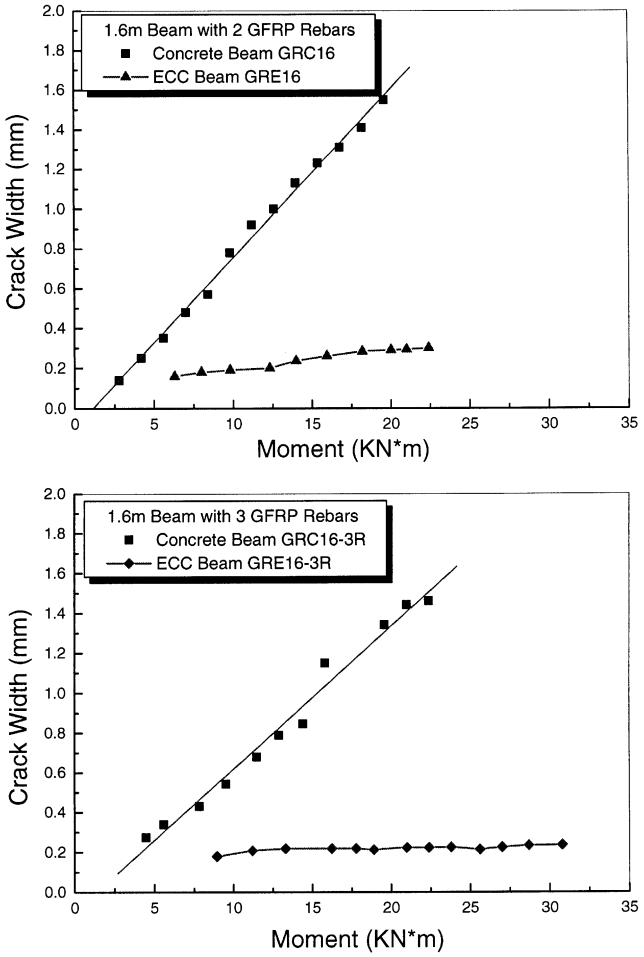

Fig. 12—Crack width versus maximum applied moment curves.

stiffness of GFRP-reinforced concrete beams in a cracked state, the deflection and, in turn, the crack width at service load generally are much larger than those of equivalent steel-reinforced beams.[23,24] As mentioned in the introduction, the serviceability limits, therefore, would govern the design of FRP-reinforced structural members. For FRP-reinforced concrete members, the maximum crack width limit would mainly be governed by leakage control or freezing-and-thawing resistance rather than corrosion consideration. Excessive crack width, especially in the case of members with low reinforcement ratios, however, is not acceptable. As shown in Fig. 6, 8, and 10, several large cracks formed in GFRP reinforced concrete beams. In contrast, numerous fine cracks developed in the ECC beams. The average crack spacing of ECC beams is approximately one order of magnitude lower. Figure 11 shows the different patterns of shear cracking, which led to final failure in concrete Beam GRC10 and ECC Beam GRE10. These two beams had close shear capacity, though for GRC10 the shear strength was mainly provided by the steel stirrups, while for the latter, shear capacity was provided by the ECC matrix. For the concrete beam, only two wide cracks formed within the shear span, accompanied by surface spalling of the concrete, while for the ECC beam, more than 40 cracks were observed, and the ECC cover remained intact after failure.

Figure 12 presents the average crack width measured at the constant moment span versus maximum applied moment for both the concrete beam and the ECC beam in Series II and III. All of the beams had shear reinforcement. In general, a higher reinforcement ratio leads to lower crack widths at the same applied moment. For concrete beams, as pointed out by numerous researchers,[3,9,12] crack width increases almost linearly with moment (to over 1.4 mm before peak load), while for ECC beams, the increase of crack width slows down with the increase of applied moment and finally stabilizes to less than 0.3 mm. This was also observed in a related study by Maalej and Li.[25] The significant difference in crack width development derives from the difference in the cracking process of these two matrixes. For the concrete beam, cracking occurs as a tension-softening process so that the crack opens with decreasing traction. For the ECC matrix, cracking occurs as a damage process when the composite strain-hardens. Further details on the contrast between tension-softening fracture process and microcrack damage process can be found in Reference 26. The strain capacity of the ECC used is 3.5%, higher than that of the GFRP rod (1.9%). During strain hardening, the microcracks in the ECC open with increasing traction.

Another issue related to cracking is the stress concentration acting on the reinforcing bar across the crack face. Once the concrete beam cracks, the stress carried by the matrix transfers to the reinforcing bar. The resulting stress concentration causes debonding to take place at the reinforcing bar and concrete interface. The reinforcing bar stress at the crack face may be expected to be higher than the average stress along the whole reinforcing bar. The magnitude of this stress difference depends on the reinforcement ratio, concrete tensile strength and modulus, and interface properties. When the reinforcing bar stress at the crack face reaches its strength capacity, the reinforcing bar breaks. Therefore, for concrete members, the elongation capacity of FRP reinforcing bars cannot be fully utilized due to localized stress concentration.

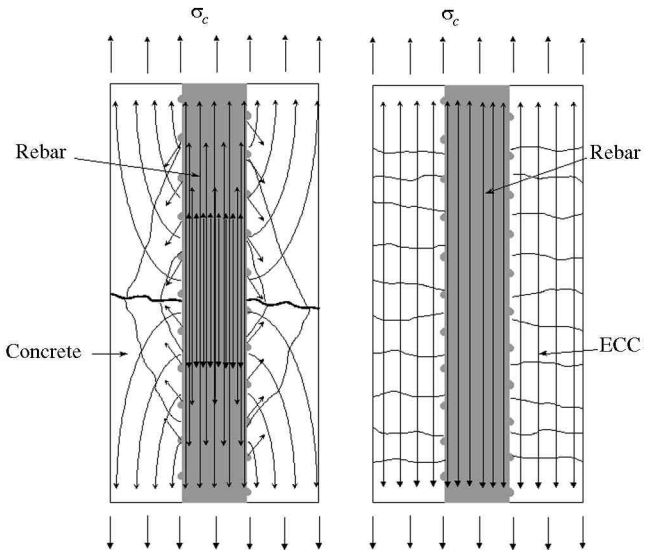

Fig. 13—Stress distribution in cracked reinforcement members under tension: (left) in concrete members, there is stress concentration in reinforcing bar at crack vicinity; (right) in ECC members, stress is uniformly distributed in ECC matrix and in reinforcing bar.

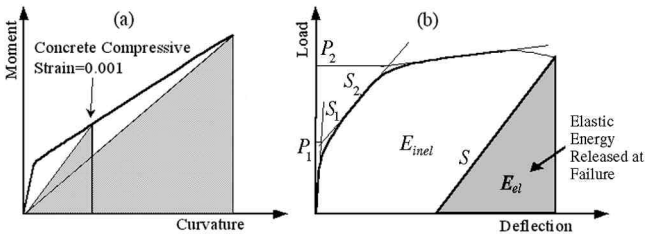

Fig. 14—Two approaches to defining ductility index for FRP-reinforced members: (a) based on deformability; and (b) based on energy ratio.

Nevertheless, for regular concrete members, this deformation reduction may be alleviated by weak bonding between the GFRP reinforcing bar and the matrix. Because the cracking takes place at a very early stage of loading, in the context of practically used reinforcement ratios, the stress jump on the reinforcing bar may be moderate. Moreover, the ultimate strain of FRP material usually is one order of magnitude higher than the yielding strain of steel; FRP reinforcing bar possesses a sufficient deformation margin. Large slippage between the reinforcing bar and the matrix may introduce secondary longitudinal splitting cracks and further smear the stress concentration on the reinforcing bar. In the case of FRP prestressed concrete members, however, the situation may be severely aggravated. Because a large amount of strain capacity of the FRP tendon is utilized by prestressing, the impact of a stress jump on the tendon due to cracking can become considerable. For a fully bonded tendon, the reduction in GFRP deformation capacity is rather evident. This issue, however, is beyond the scope of this paper.

The scenario is essentially different for reinforced ECC members, as illustrated in Fig. 13. Because of strain hardening and its large strain capacity, the ECC matrix can deform compatibly with the reinforcing bar. There is basically no shear lag existing between the reinforcing bar and the matrix, and the stress concentration on the reinforcing bar is nonexistent even when the ECC is experiencing microcrack damage. In a preliminary study conducted by Li and Fischer[27] on the tensile behavior of steel reinforcing bar-reinforced ECC members in the form of tension-stiffening specimens, they observed that, macroscopically, the yielding of steel reinforcing bars was delayed in the ECC matrix compared with those in the concrete matrix. Strain jumps were measured locally (by strain gages attached in the reinforcing bar) whenever concrete cracked, but were not observed in the reinforced ECC elements. The test results of Series II show that ECC beams do achieve moderate improvement in deflection and moment capacity, which suggests the validity of the aforementioned assertion.

It should be pointed out that, as a material specially tailored based on micromechanical models, the crack spacing and density can be controlled.[28] It has been demonstrated how ECC materials can be used as a cover layer for a concrete flexural member to control crack width.[29] When strain-hardening ECC materials replace concrete as the matrix of FRP-reinforced members, the serviceability limit of crack width would not govern the design of a flexural member.

Deformability and ductility

Ductility describes the ability of structural members to sustain inelastic deformation prior to failure without significant loss in load-carrying capacity.[30] To ensure the safety of a structural member under overload, two essential performance features are required. First, the structural member should be able to undergo large deformations and associated wide cracks prior to collapse, so that an overload can be easily detected. Second, high inelastic energy absorption while maintaining load capacity is preferred to avoid elastic-brittle catastrophic failure. In recognition of this, ductility can be expressed in terms of deformation or of energy absorption. In the case of conventional steel-reinforced members, ductility can be measured as the ratio of deformation at ultimate state to the deformation at yielding of the main reinforcement. This definition of ductility is obviously not suitable for FRP-reinforced members, wherein a clear yielding point of the reinforcing bar does not exist. Several authors have addressed this problem, but there is no general agreement on the definition of ductility of FRP-reinforced structural members.[3,5,22,31]

In 1995, Jaeger, Mufti, and Tadros proposed an index based on deformability to evaluate the ductility of FRP-reinforced concrete beams.[31] This index, which is also known as the J-factor, takes into account the increase of moment as well as the increase of deformation, and is defined as the product of moment factor and curvature factor. The moment factor and curvature factor are, in turn, defined as the ratios of moment and curvature at ultimate state to those at a concrete compressive strain of 0.001. This definition of ductility can be interpreted as the safety margin of structural members. The state when the concrete compressive strain reaches 0.001 is considered the beginning of inelastic deformation of concrete, and is regarded as the equivalent point of structural yielding. In the case of members with perfect elastic response up to failure, the J-factor represents the ratio of stored energy at ultimate state to that of a reference point, as shown in Fig. 14(a). A low limit of 4 was recommended by Jaeger, Mufti, and Tadros when the J-factor was used to measure the safety of FRP-reinforced members. In a study by Theriault and Benmokrane, all of the 12 simple concrete beams reinforced by GFRP rods yielded J-factors greater than 6, and were considered safe for design based on the considerations of

Table 4—Summary of test results

Series	Beam designation	Peak load, kN	Ultimate deflection, mm	Fracture energy, J	Energy dissipation ratio, %	Failure mode
I	SRC10	75.6	31.2	2122	95.0	Flexural-tension
	GRC10-ns	34.7	4.7	123	—	Shear
	GRC10	90.7	15.1	582	35.9	Shear-compression
	GRE10-ns	86.9	20.2	2031	79.0	Shear-tension
		89.6	16.0	2003	62.3	
	GRE10	132.7	23.7	2014	47.5	Shear
		134.1	23.2	2041	47.1	
II	GRC16	62.1	37.4	1377	40.4	Flexural-tension
	GRE16-ns	77.4	46.3	2592	43.5	Shear
	GRE16	73.8	43.8	1898	38.4	Flexural-tension
		76.9	43.3	2016	39.0	
III	GRC16-3R	69.7	31.5	2241	30.3	Flexural-compression
		75.4	33.4	1679	44.3	
	GRC16-3R-ns	83.5	33.1	2875	32.6	Shear
	GRC16-3R	106.9	48.2	3349	42.6	Flexural-compression
		104.6	46.8	3384	46.0	

strength and deformability.[3] The research of Vijay, Kumar, and GangaRao showed that FRP-reinforced beams with low reinforcement ratios that failed in tensile rupture of FRP rods have larger J-factors than those beams that failed in compression,[32] even though the compression failure was more ductile and gradual than tensile rupture. A direct application of the J-factor to ECC beams in this study is questionable. Because there is 40 to 100% improvement in compression strain capacity for ECC materials, as well as relatively lower modulus of elasticity,[33] the direct comparison of J-factors between ECC beams and concrete beams is not convincing. For instance, the J-factors of GRC16 and GRC16-3R are 7.66 and 7.42 respectively, whereas they are 24.5 and 31.7 for GRE16 and GRE16-3R, respectively. In fact, for beams with similar geometry but different materials, the fracture energy, which is defined as the area under the load-deflection curve, could be considered an equivalent, but more reasonable, measurement to the deformability-based ductility index.

FRP-reinforced members generally perform satisfactorily in deformation capacity, where the most absorbed energy is elastic energy. Considering that the ability of energy dissipation in an inelastic way was the essential component of structural ductility, Naaman and Jeong proposed a new definition of the ductility index in 1995, which was expressed as the ratio relating any two of the inelastic, elastic, and total energies.[5] A simple energy dissipation index expressed as the ratio of the inelastic energy E_{inel} to the total energy $E_{inel} + E_{el}$ is considered herein, as illustrated in Fig. 14(b). Herein, the failure point is defined as the point where the load drops to 85% of the peak load. The elastic energy can be separated from the total energy by unloading and reloading tests, or can be estimated from the area of the triangle determined by the line with the weighted average slope of the two initial straight lines of the load-deflection curve. The slope S is given by

$$S = \frac{P_1 S_1 + (P_2 - P_1) S_2}{P_2} \quad (1)$$

where P_1 and P_2 are loads and S_1 and S_2 are corresponding slopes. There is no prerequisite for the application of this definition of ductility, whatever the failure mode, to materials or reinforcement configurations.

Table 4 gives the summary of test results as well as the fracture energy and energy dissipation ratio of each beam. Except for GRC10 and GRC10-ns, the elastic energy of the other beams is decided by drawing a line parallel to the unloading branch at the failure point, while for GRC10, it was estimated by using Eq. (1).

In general, ECC beams behave more ductilely than concrete beams based on either the total fracture energy or the inelastic energy dissipation ability, but the magnitude of improvement strongly depends on the failure modes. When shear resistance dominates structural capacity, for example, in Series I, the use of ECC matrix leads to dramatic improvements in fracture energy and inelastic energy dissipation ratio. For instance, the fracture energies of ECC beams GRE10 and GRE10-ns are about 3.5 times that of concrete beam GRC10, and their inelastic energy dissipation ratios are 1.3 and 2 times that of beam GRC10, respectively. It was also noticed that, although the fracture energy is quite similar between two types of ECC beams, there is significant difference in how this energy is stored. For the ECC beam without stirrups GRE10-ns, most energy dissipated by the means of large shear deformation, while for the ECC beam with stirrups GRE10, larger portions of the absorbed energy were elastically stored where the matrix shear deformation was restrained by the shear reinforcement (less fiber pullout, for example). The ductility of beam GRE10-ns is comparable to steel-reinforced reference beam SRC10. When the structural limit state is governed by flexural bending failure, beams failed in compression (such as those in Series III) benefit more from the ECC matrix than those failed in tension (Series II). For instance, the fracture energy and dissipation ratio of ECC beam GRE16-3R are 70 and 20% higher, respectively, than those of concrete beam GRC16-3R; in comparison, the fracture energy of GRE16 is about 40% higher than that of GRC16 and shows no improvement in terms of dissipation ratio.

FURTHER DISCUSSION

Large reinforcement ratios are typically used in FRP-reinforced members for deflection control; therefore, flexural tension failure is inhibited and the member is more vulnerable

to shear failure, as mentioned in the introduction. For sections subjected to shear and bending simultaneously, shear failure may be caused by the rupture or yielding (in the case of steel) of shear reinforcement, or by compressive failure of the diagonal compression section of the concrete. The failure mode of the former is very brittle because FRP reinforcing bars have very low strength to resist shear deformation acting orthogonally on them and resulting in immediate rupture of the longitudinal reinforcement. As for the latter, similarly to flexural compressive failure, a certain amount of deformation may occur. Consequently, compressive failure associated with the over-reinforced design concept becomes the preferable limit state for FRP-reinforced concrete members. The level of ductility achievable with over-reinforced beams, however, depends on the confinement provided in the compressive zone. For HSC, intensive spirals or stirrups have to be installed.

For FRP-reinforced ECC beams, at the level of section, the over-reinforced design concept is still valid. The present study, however, reveals that shear failure can be an appealing structural limit state due to the ductile nature of ECC. In particular, the shear–tension failure mode demonstrates a pseudoyielding plateau similar to that of steel-reinforced members (Fig. 5). When the shear capacity of the ECC matrix itself can provide significant structural resistance, crowded shear reinforcement, which is usually required in equivalent concrete members, becomes unnecessary.

The classical method for predicting the shear strength and failure mode under combined shearing and bending load may be questionable. Although the compressive strength of the concrete and ECC matrixes used in this investigation have comparable values, there is a significant difference in the shear strength between two pairs of beams: GRC10-ns (1.77 MPa, calculated by $1.5V_u/(b \cdot d)$, where V_u is the ultimate shear load, b is the beam width, and d is the depth of longitudinal reinforcement) versus GRE10-ns (2.95 MPa), and GRC10 (3.08 MPa) versus GRE10 (4.51 MPa). This suggests that the conventional equations presented in design codes for computing shear capacity, which directly relate the shear strength to the matrix compressive strength, are no longer valid for ECC beams.

In order to predict the limit state and ductility of FRP-reinforced ECC beams, further theoretical and experimental work is needed to develop more sophisticated models based on fracture mechanics and material constitutive laws. Preliminary analysis work can be found in Reference 34, wherein the load and deflection limits of various FRP-reinforced ECC flexural members have been analyzed.

CONCLUSIONS

Experimental investigation and theoretical prediction of the flexural behaviors of HSC beams and ECC beams are presented in this paper. Three series, totaling 11 different types of beams (10 with GFRP reinforcements) with various shear span-depth and longitudinal reinforcement ratios, designed for different targeted failure modes, were tested under static loading conditions. In general, large deformations were observed for both concrete beams and ECC beams. With the same reinforcement configuration, however, ECC beams exhibit significantly larger deflections and load-carrying capacities than do the counterpart HSC beams. The extent of improvement strongly depends on the dominating failure mode. When structural failure is controlled by flexural tension capacity, that is, for an under-reinforced section, the benefit of the ECC matrix in terms of the deformability and energy dissipation is marginal. For cases failing in shear or in compression, however, where the matrix performance dominates the ultimate limit state, the positive effect of using ECC matrix is significant. Pseudoyielding plateaus were observed, particularly in the case of the ECC beam that failed in shear tension.

When it is evident that the use of ductile-matrix ECC can improve the structural ductility of FRP-reinforced members, change in design concepts becomes necessary. In order to translate the material ductility successfully into structural ductility, at the level of section, over-reinforced design is preferable. For ECC beams with short shear span-depth ratios, shear failure as the ultimate limit state, which is usually deliberately avoided in the case of concrete short beams, is allowable, even encouraged.

Reflecting superior tensile strength and strain capacity, ECC exhibits remarkable shear resistance. For beams of the tested geometry, the ECC beam without shear reinforcement shows even better flexural stiffness, ductility, and load-carrying capacity than the similar HSC beam with dense steel stirrups, indicating that eliminating shear reinforcement is feasible when using ECC matrix.

The strain-hardening and multiple-cracking behaviors of ECC material also change its cracking pattern. Instead of large opening cracks observed on concrete beams, numerous small cracks develop on ECC beams. While the crack width of concrete beams increases linearly with load, that of ECC beams keeps almost constant up to failure. At the limit state, the crack width in ECC beams is about one-seventh of that in concrete beams; therefore, the serviceability limit of crack width control will no longer govern the design of flexural members. The noncorrosive nature of the FRP reinforcement and the small crack width of the ECC matrix should enhance durability in such reinforced ECC structures.

As two relatively new civil engineering materials, ECC and FRP each possess unique and desirable features. In the era of moving toward performance-based design approaches, structural members made by appropriate combinations of these new materials can meet higher performance demands that may be difficult to satisfy with conventional steel-reinforced concrete members. Toward this end, this paper presents the results of a preliminary investigation; further research is needed to more effectively translate material performance to structural performance.

ACKNOWLEDGMENTS

This project has been supported by a National Science Foundation grant (CMS-9601262) to the University of Michigan. Helpful discussions with Gregor Fischer and Jun Zhang are gratefully acknowledged. The authors would also like to thank Hughes Brothers, Inc., which supplied the GFRP reinforcements for this study.

REFERENCES

1. Fukuyama, H. et al., "Structural Performances of Concrete Frame Reinforced With FRP Reinforcement," *Non-Metallic (FRP) Reinforcement of Concrete Structures*, L. Taerwe, ed., E&FN Spon, London, 1995, pp. 379-386.

2. ACI Committee 440, "State-of-the-Art Report on Fiber Reinforced Plastic (FRP) Reinforcement for Concrete Structures (ACI 440R-96)," American Concrete Institute, Farmington Hills, Mich., 1996, 68 pp.

3. Sonobe, Y. et al., "Design Guidelines of FRP Reinforced Concrete Building Structures," *Journal of Composites for Construction*, V. 1, No. 3, Aug. 1997, pp. 90-113.

4. Theriault, M., and Benmokrane, B., "Effect of FRP Reinforcement Ratio and Concrete Strength on Flexural Behavior of Concrete Beams," *Journal of Composites for Construction*, V. 2, No. 1, Feb. 1998, pp. 7-15.

5. Naani, A., "Flexural Behavior and Design of RC Members Using FRP Reinforcement," *Journal of Structural Engineering*, V. 119, No. 11, Nov. 1993, pp. 3344-3359.

6. Naaman, A. E., and Jeong, S. M., "Structural Ductility of Concrete Beams Prestressed with FRP Tendons," *Non-Metallic (FRP) Reinforcement of Concrete Structures*, L. Taerwe, ed., E&FN Spon, London, 1995, pp. 379-386.

7. Tamuzs, V., and Tepfers, R., "Ductility of Non-Metallic Hybrid Fiber Composite Reinforcement for Concrete," *Non-Metallic (FRP) Reinforcement of Concrete Structures*, L. Taerwe, ed., E&FN Spon, London, 1995, pp. 18-25.

8. Harris, H. G.; Somboonsong, W.; and Ko, F. K., "New Ductile Hybrid FRP Reinforcing Bar for Concrete Structures." *Journal of Composites for Construction*, V. 2, No. 1, Feb. 1998, pp. 28-37.

9. Nawy, E. G.; Neuwerth, G. E.; and Philips, C. J., "Behavior of Fiber Glass Reinforced Concrete Beams," *ASCE Journal of the Structural Division*, V. 97, No. ST9, 1971, pp. 2203-2215.

10. Nawy, E. G., and Neuwerth, G. E., "Fiberglass Reinforced Concrete Slabs and Beams," *ASCE Journal of the Structural Division*, V. 103, No. ST2, 1977, pp. 421-428.

11. Faza, S. S., and GangaRao, H. V. S., "Theoretical and Experimental Correlation of Behavior of Concrete Beams Reinforced with Fiber Reinforced Plastic Rebars," *Fiber-Reinforced-Plastic Reinforcement for Concrete Structures: Proceedings of International Symposium*, SP-138, A. Nanni and C. W. Dolan, eds., American Concrete Institute, Farmington Hills, Mich., 1993, pp. 599-614.

12. Benmokrane, B.; Chaallal, O.; and Masmoudi, R, "Flexural Response of Concrete Beams Reinforced with FRP Reinforcing Bars," *ACI Structural Journal*, V. 93, No. 1, Jan.-Feb. 1996, pp. 46-55.

13. Mikami, H.; Hatoh, H.; Takeuchi, H.; and Tamura, T., "Flexural and Shear Behavior of RC Beams Reinforced with FRP Rods in Spiral Shape," *Transactions of the Japanese Concrete Institute*, Tokyo, Japan, No. 1, 1989, pp. 199-206.

14. Ueda, T.; Sato, Y.; Kakuta, Y.; Imamura, A.; and Kanematsu, H., "Failure Criteria for FRP Rods Subjected to a Combination of Tension and Shear Forces," *Non-Metallic (FRP) Reinforcement of Concrete Structures*, L. Taerwe, ed., E&FN Spon, London, 1995, pp. 26-33.

15. Li, V. C., "Engineered Cementitious Composites—Tailored Composites through Micromechanical Modeling," *Fiber Reinforced Concrete: Present and the Future*, N. Banthia; A. Bentur; and A. Mufti, eds., Canadian Society of Civil Engineers, Montreal, 1998, pp. 64-97.

16. Maalej, M.; Hashida, T.; and Li, V. C., "Effect of Fiber Volume Fracture on the Off-Crack-Plane Fracture Energy in Strain-Hardening Engineered Cementitious Composites," *Journal of the American Ceramic Society*, V. 78, No. 12, 1995, pp. 3369-3375.

17. Li, V. C., and Maalej, M., "Toughening in Cement Based Composites, Part 2: Fiber Reinforced Cementitious Composites," *Journal of Cement and Concrete Composites*, V. 18, No. 4, 1996, pp. 239-249.

18. Fukuyama, H.; Sato, Y.; Li, V. C.; Matsuzaki, Y.; and Mihashi, H., "Ductile Engineered Cementitious Composite Elements for Seismic Structural Application," *Proceedings of the 12th World Conference on Earthquake Engineering*, Auckland, New Zealand, 2000.

19. Li, V. C., "From Micromechanics to Structural Engineering—The Design of Cementitious Composites for Civil Engineering Application," *JSCE Journal of Structural Mechanics and Earthquake Engineering*, V. 10, No. 2, 1993, pp. 37-48.

20. Li, V. C., "Repair and Retrofit with Engineered Cementitious Composites," *Fracture Mechanics of Concrete Structures*, AEDIFICATID, Freiburg, Germany, 1998, pp. 1715-1726.

21. Li, V. C.; Wu, H. C.; Maalej, M.; and Mishra, D. K., "Tensile Behavior of Cement-Based Composites with Random Distributed Steel Fibers," *Journal of the American Ceramic Society*, V. 79, No. 1, 1996, pp. 74-78.

22. ACI Committee 318, "Building Code Requirements for Structural Concrete (ACI 318-95) and Commentary (318R-95)," American Concrete Institute, Farmington Hills, Mich., 1995, 369 pp.

23. Grace, N. F.; Soliman, A. K.; Abdel-Sayed, G.; and Saleh, K. R., "Behavior and Ductility of Simple and Continuous FRP Reinforced Beams," *Journal of Composites for Construction*, V. 2, No. 4, Nov. 1998, pp. 186-194.

24. Nakano, K.; Matsuzaki, Y.; Fukuyama, H.; and Teshigawara, M., "Flexural Performance of Concrete Beams Reinforced with Continuous Fiber Bars," *Fiber-Reinforced-Plastic Reinforcement for Concrete Structures: Proceedings of International Symposium*, SP-138, A. Nanni and C. W. Dolan, eds., American Concrete Institute, Farmington Hills, Mich., 1993, pp. 743-766.

25. Maalej, M., and Li, V. C., "Introduction of Strain-Hardening Engineered Cementitious Composites in Design of Reinforced Concrete Flexural Members for Improved Durability," *ACI Structural Journal*, V. 92, No. 2, Mar.-Apr. 1995, pp. 167-176.

26. Li, V. C., "When a Crack Is Not a Crack," *Proceedings of Brittle Matrix Composites 6*, A. Brandt, V. C. Li, and I. Marshall, eds., ZTUREK RSI and Woodhead Publishing, Warsaw, Poland, 2000, pp. 173-185.

27. Li, V. C., and Fischer, G., "Interaction between Steel Reinforcement and Engineered Cementitious Composites," *Proceedings, High Performance Fiber Reinforced Cement Composites 3*, H. W. Reinhardt and A. Naaman, eds., Chapman & Hull, May 1999, pp. 361-370.

28. Li, V. C.; Mishra, D. K; and Wu, H.C, "Matrix Design for Pseudo-Strain Hardening Fiber Reinforced Cementitious Composites," *Journal of Materials and Structures*, RILEM, V. 28, No. 183, 1995, pp. 586-589.

29. Maalej, M., and Li, V. C., "Flexural/Tensile-Strength Ratio in Engineered Cementitious Composites," *Journal of Materials in Civil Engineering*, V. 6, No. 4, 1994, pp. 513-528.

30. Naaman, A. E.; Harajli, M. H.; and Wight, J. K., "Analysis of Ductility in Partially Prestressed Concrete Flexural Members," *PCI Journal*, V. 31, No. 3, 1986, pp. 64-87.

31. Jaejer, L. G.; Mufti, A. A.; and Tadros, G, "The Concept of the Overall Performance Factor in Rectangular-Section Reinforced Concrete Beams," *Proceedings of the 3rd International Symposium on Non-Metallic (FRP) Reinforcement for Concrete Structures*, V. 2, pp. 551-558.

32. Vijay, P. V.; Kumar, S. V.; and GangRao, H. V. S., "Shear and Ductility Behavior of Concrete Beams Reinforced by GFRP Rebars," *Proceedings of the 2nd Conference on Advanced Composite Materials in Bridges and Structures*, M. El-Badry, ed., Canadian Society for Civil Engineering, Montreal, Canada, 1996, pp. 217-226.

33. Misha, D. K., "Design of Pseudo Strain-Hardening Cementitious Composites for a Ductile Plastic Hinge," PhD thesis, Department of Civil and Environmental Engineering, University of Michigan, Ann Arbor, 1995, pp. 107-109.

34. Fischer, G., and Li., V. C., "Deformation Behavior of FRP Reinforced ECC Flexural Member under Reversed Cyclic Loading Conditions." (submitted for publication)